Online Appendix for

Dynamic Prediction Pools: An Investigation of Financial Frictions and Forecasting Performance

Marco Del Negro, Raiden B. Hasegawa, and Frank Schorfheide

This appendix consists of the following sections:

A Detailed Description of DSGE Models

A.1 Model 1: The Smets-Wouters Model with Time-Varying Inflation Target (SWπ)

Model Specification. We use a slightly modified version of the Smets and Wouters (2007) model. Following Del Negro and Schorfheide (2013), we detrend the non-stationary model variables by a stochastic rather than a deterministic trend. This approach makes it possible to express almost all equilibrium conditions in a way that encompasses both the trend-stationary total factor productivity process in Smets and Wouters (2007), as well as the case where technology follows a unit root process. Let $\tilde{z}_t$ be the linearly detrended log productivity process which follows the autoregressive law of motion

$$\tilde{z}_t = \rho_z \tilde{z}_{t-1} + \sigma_z \varepsilon_{z,t}. \tag{A-1}$$

We detrend all non stationary variables by $Z_t = e^{\gamma t + \frac{1}{1-\alpha}\tilde{z}_t}$, where γ is the steady state growth rate of the economy. The growth rate of Z_t in deviations from γ, denoted by z_t, follows the process:

$$z_t = \ln(Z_t/Z_{t-1}) - \gamma = \frac{1}{1-\alpha}(\rho_z - 1)\tilde{z}_{t-1} + \frac{1}{1-\alpha}\sigma_z \epsilon_{z,t}. \tag{A-2}$$

All variables in the following equations are expressed in log deviations from their non-stochastic steady state. Steady state values are denoted by $*$-subscripts and steady state formulas are provided in the technical appendix of Del Negro and Schorfheide (2013). The consumption Euler equation is given by:

$$\begin{aligned} c_t = &-\frac{(1-he^{-\gamma})}{\sigma_c(1+he^{-\gamma})}\left(R_t - \mathbb{E}_t[\pi_{t+1}] + b_t\right) + \frac{he^{-\gamma}}{(1+he^{-\gamma})}\left(c_{t-1} - z_t\right) \\ &+ \frac{1}{(1+he^{-\gamma})}\mathbb{E}_t\left[c_{t+1} + z_{t+1}\right] + \frac{(\sigma_c - 1)}{\sigma_c(1+he^{-\gamma})}\frac{w_* L_*}{c_*}\left(L_t - \mathbb{E}_t[L_{t+1}]\right), \end{aligned} \tag{A-3}$$

where c_t is consumption, L_t is labor supply, R_t is the nominal interest rate, and π_t is inflation. The exogenous process b_t drives a wedge between the intertemporal ratio of the marginal utility of consumption and the riskless real return $R_t - \mathbb{E}_t[\pi_{t+1}]$, and follows an AR(1) process with parameters ρ_b and σ_b. The parameters σ_c and h capture the degree of relative risk aversion and the degree of habit persistence in the utility function, respectively. The following condition expresses the relationship between the value of capital in terms of consumption q_t^k and the level of investment i_t measured in terms of consumption goods:

$$q_t^k = S'' e^{2\gamma}(1+\bar{\beta})\Big(i_t - \frac{1}{1+\bar{\beta}}\left(i_{t-1} - z_t\right) - \frac{\bar{\beta}}{1+\bar{\beta}} \mathbb{E}_t\left[i_{t+1} + z_{t+1}\right] - \mu_t\Big), \tag{A-4}$$

which is affected by both investment adjustment cost (S'' is the second derivative of the adjustment cost function) and by μ_t, an exogenous process called the "marginal efficiency of investment" that affects the rate of transformation between consumption and installed capital. The exogenous process μ_t follows an AR(1) process with parameters ρ_μ and σ_μ. The parameter $\bar{\beta} = \beta e^{(1-\sigma_c)\gamma}$ depends on the intertemporal discount rate in the utility function of the households β, the degree of relative risk aversion σ_c, and the steady-state growth rate γ.

The capital stock, $\bar{k}_t$, evolves as

$$\bar{k}_t = \left(1 - \frac{i_*}{\bar{k}_*}\right)\left(\bar{k}_{t-1} - z_t\right) + \frac{i_*}{\bar{k}_*} i_t + \frac{i_*}{\bar{k}_*} S'' e^{2\gamma}(1+\bar{\beta})\mu_t, \tag{A-5}$$

where $i_*/\bar{k}_*$ is the steady state ratio of investment to capital. The arbitrage condition between the return to capital and the riskless rate is:

$$\frac{r_*^k}{r_*^k + (1-\delta)} \mathbb{E}_t[r_{t+1}^k] + \frac{1-\delta}{r_*^k + (1-\delta)} \mathbb{E}_t[q_{t+1}^k] - q_t^k = R_t + b_t - \mathbb{E}_t[\pi_{t+1}], \tag{A-6}$$

where r_t^k is the rental rate of capital, r_*^k its steady state value, and δ the depreciation rate. Given that capital is subject to variable capacity utilization u_t, the relationship between $\bar{k}_t$ and the amount of capital effectively rented out to firms k_t is

$$k_t \;=\; u_t - z_t + \bar{k}_{t-1}. \tag{A-7}$$

The optimality condition determining the rate of utilization is given by

$$\frac{1-\psi}{\psi} r_t^k = u_t, \tag{A-8}$$

where ψ captures the utilization costs in terms of foregone consumption. Real marginal costs for firms are given by

$$mc_t \;=\; w_t + \alpha L_t - \alpha k_t, \tag{A-9}$$

where w_t is the real wage and α is the income share of capital (after paying markups and fixed costs) in the production function. From the optimality conditions of goods producers it follows that all firms have the same capital-labor ratio:

$$k_t \;=\; w_t - r_t^k + L_t. \tag{A-10}$$

The production function is:

$$y_t = \Phi_p \left(\alpha k_t + (1-\alpha) L_t\right) + \mathcal{I}\{\rho_z < 1\}(\Phi_p - 1)\frac{1}{1-\alpha}\tilde{z}_t, \tag{A-11}$$

if the log productivity is trend stationary. The last term $(\Phi_p - 1)\frac{1}{1-\alpha}\tilde{z}_t$ drops out if technology has a stochastic trend, because in this case one has to assume that the fixed costs are proportional to the trend. Similarly, the resource constraint is:

$$y_t = g_t + \frac{c_*}{y_*}c_t + \frac{i_*}{y_*}i_t + \frac{r_*^k k_*}{y_*}u_t - \mathcal{I}\{\rho_z < 1\}\frac{1}{1-\alpha}\tilde{z}_t, \tag{A-12}$$

where again the term $-\frac{1}{1-\alpha}\tilde{z}_t$ disappears if technology follows a unit root process. Government spending g_t is assumed to follow the exogenous process:

$$g_t = \rho_g g_{t-1} + \sigma_g \varepsilon_{g,t} + \eta_{gz}\sigma_z\varepsilon_{z,t}.$$

Finally, the price and wage Phillips curves are, respectively:

$$\pi_t = \frac{(1-\zeta_p\bar{\beta})(1-\zeta_p)}{(1+\iota_p\bar{\beta})\zeta_p((\Phi_p - 1)\epsilon_p + 1)}mc_t + \frac{\iota_p}{1+\iota_p\bar{\beta}}\pi_{t-1} + \frac{\bar{\beta}}{1+\iota_p\bar{\beta}}\mathbb{E}_t[\pi_{t+1}] + \lambda_{f,t}, \tag{A-13}$$

and

$$\begin{aligned} w_t = {} & \frac{(1-\zeta_w\bar{\beta})(1-\zeta_w)}{(1+\bar{\beta})\zeta_w((\lambda_w - 1)\epsilon_w + 1)}\left(w_t^h - w_t\right) - \frac{1+\iota_w\bar{\beta}}{1+\bar{\beta}}\pi_t + \frac{1}{1+\bar{\beta}}\left(w_{t-1} - z_t - \iota_w\pi_{t-1}\right) \\ & + \frac{\bar{\beta}}{1+\bar{\beta}}\mathbb{E}_t\left[w_{t+1} + z_{t+1} + \pi_{t+1}\right] + \lambda_{w,t}, \end{aligned} \tag{A-14}$$

where ζ_p, ι_p, and ϵ_p are the Calvo parameter, the degree of indexation, and the curvature parameter in the Kimball aggregator for prices, and ζ_w, ι_w, and ϵ_w are the corresponding parameters for wages. w_t^h measures the household's marginal rate of substitution between consumption and labor, and is given by:

$$w_t^h = \frac{1}{1-he^{-\gamma}}\left(c_t - he^{-\gamma}c_{t-1} + he^{-\gamma}z_t\right) + \nu_l L_t, \tag{A-15}$$

where ν_l characterizes the curvature of the disutility of labor (and would equal the inverse of the Frisch elasticity in absence of wage rigidities). The mark-ups $\lambda_{f,t}$ and $\lambda_{w,t}$ follow exogenous ARMA(1,1) processes

$$\lambda_{f,t} = \rho_{\lambda_f}\lambda_{f,t-1} + \sigma_{\lambda_f}\varepsilon_{\lambda_f,t} + \eta_{\lambda_f}\sigma_{\lambda_f}\varepsilon_{\lambda_f,t-1}, \text{ and}$$

$$\lambda_{w,t} = \rho_{\lambda_w} \lambda_{w,t-1} + \sigma_{\lambda_w} \varepsilon_{\lambda_w,t} + \eta_{\lambda_w} \sigma_{\lambda_w} \varepsilon_{\lambda_w,t-1},$$

respectively. Finally, the monetary authority follows a generalized feedback rule:

$$\begin{aligned} R_t &= \rho_R R_{t-1} + (1-\rho_R)\Big(\psi_1 \pi_t + \psi_2 (y_t - y_t^f)\Big) \\ &\qquad + \psi_3 \Big((y_t - y_t^f) - (y_{t-1} - y_{t-1}^f)\Big) + r_t^m, \end{aligned} \quad \text{(A-16)}$$

where the flexible price/wage output y_t^f is obtained from solving the version of the model without nominal rigidities (that is, Equations (A-3) through (A-12) and (A-15)), and the residual r_t^m follows an AR(1) process with parameters ρ_{r^m} and σ_{r^m}.

In order to capture the rise and fall of inflation and interest rates in the estimation sample, we replace the constant target inflation rate by a time-varying target inflation. The interest-rate feedback rule of the central bank (A-16) is modified as follows

$$\begin{aligned} R_t &= \rho_R R_{t-1} + (1-\rho_R)\Big(\psi_1 (\pi_t - \pi_t^*) + \psi_2 (y_t - y_t^f)\Big) \\ &\quad + \psi_3 \Big((y_t - y_t^f) - (y_{t-1} - y_{t-1}^f)\Big) + r_t^m. \end{aligned} \quad \text{(A-17)}$$

The time-varying inflation target evolves according to:

$$\pi_t^* = \rho_{\pi^*} \pi_{t-1}^* + \sigma_{\pi^*} \epsilon_{\pi^*,t}, \quad \text{(A-18)}$$

where $0 < \rho_{\pi^*} < 1$ and $\epsilon_{\pi^*,t}$ is an iid shock. We model π_t^* as following a stationary process, although our prior for ρ_{π^*} will force this process to be highly persistent. A detailed justification of this modification of the policy rule is provided in Del Negro and Schorfheide (2013).

Model Solution and State-Space Representation. We use the method in Sims (2002) to solve the log-linear approximation of the DSGE model. We collect all the DSGE model parameters in the vector θ, stack the structural shocks in the vector ϵ_t, and derive a state-space representation for our vector of observables y_t. The state-space representation is comprised of the transition equation:

$$s_t = \mathcal{T}(\theta) s_{t-1} + \mathcal{R}(\theta) \epsilon_t, \quad \text{(A-19)}$$

which summarizes the evolution of the states s_t, and the measurement equation:

$$y_t = \mathcal{Z}(\theta) s_t + \mathcal{D}(\theta), \quad \text{(A-20)}$$

which maps the states onto the vector of observables y_t, where $\mathcal{D}(\theta)$ represents the vector of steady state values for these observables.

The measurement equations for real output, consumption, investment, and real wage growth, hours, inflation, and interest rates are given by:

$$\begin{aligned}
\textit{Output growth} &= \gamma + 100\,(y_t - y_{t-1} + z_t) \\
\textit{Consumption growth} &= \gamma + 100\,(c_t - c_{t-1} + z_t) \\
\textit{Investment growth} &= \gamma + 100\,(i_t - i_{t-1} + z_t) \\
\textit{Real Wage growth} &= \gamma + 100\,(w_t - w_{t-1} + z_t)\ , \\
\textit{Hours} &= \bar{l} + 100 l_t \\
\textit{Inflation} &= \pi_* + 100\pi_t \\
\textit{FFR} &= R_* + 100 R_t
\end{aligned} \tag{A-21}$$

where all variables are measured in percent, where π_* and R_* measure the steady state level of net inflation and short term nominal interest rates, respectively and where $\bar{l}$ captures the mean of hours (this variable is measured as an index). To incorporate information about low-frequency movements of inflation the set of measurement equations (A-21) is augmented by

$$\begin{aligned}
\pi_t^{O,40} &= \pi_* + 100 \mathbb{E}_t \left[\frac{1}{40} \sum_{k=1}^{40} \pi_{t+k} \right] \\
&= \pi_* + \frac{100}{40} \mathcal{Z}(\theta)_{(\pi,.)} (I - \mathcal{T}(\theta))^{-1} \left(I - [\mathcal{T}(\theta)]^{40} \right) \mathcal{T}(\theta) s_t,
\end{aligned} \tag{A-22}$$

where $\pi_t^{O,40}$ represents observed long run inflation expectations obtained from surveys (in percent per quarter), and the right-hand-side of (A-22) corresponds to expectations obtained from the DSGE model (in deviation from the mean π_*). The second line shows how to compute these expectations using the transition equation (A-19) and the measurement equation for inflation. $\mathcal{Z}(\theta)_{(\pi,.)}$ is the row of $\mathcal{Z}(\theta)$ in (A-20) that corresponds to inflation. The SWπ model is estimated using the observables in expressions (A-21) and (A-22).

A.2 Model 2: Smets-Wouters Model with Financial Frictions (SWFF)

Model Specification. We now add financial frictions to the SW model building on the work of Bernanke et al. (1999), Christiano et al. (2003), De Graeve (2008), and Christiano et al.

(2014). In this extension, banks collect deposits from households and lend to entrepreneurs who use these funds as well as their own wealth to acquire physical capital, which is rented to intermediate goods producers. Entrepreneurs are subject to idiosyncratic disturbances that affect their ability to manage capital. Their revenue may thus be too low to pay back the bank loans. Banks protect themselves against default risk by pooling all loans and charging a spread over the deposit rate. This spread may vary as a function of the entrepreneurs' leverage and their riskiness. Adding these frictions to the SW model amounts to replacing equation (A-6) with the following conditions:

$$E_t\left[\tilde{R}^k_{t+1} - R_t\right] = b_t + \zeta_{sp,b}\left(q^k_t + \bar{k}_t - n_t\right) + \tilde{\sigma}_{\omega,t} \tag{A-23}$$

and

$$\tilde{R}^k_t - \pi_t = \frac{r^k_*}{r^k_* + (1-\delta)} r^k_t + \frac{(1-\delta)}{r^k_* + (1-\delta)} q^k_t - q^k_{t-1}, \tag{A-24}$$

where $\tilde{R}^k_t$ is the gross nominal return on capital for entrepreneurs, n_t is entrepreneurial equity, and $\tilde{\sigma}_{\omega,t}$ captures mean-preserving changes in the cross-sectional dispersion of ability across entrepreneurs (see Christiano et al. (2014)) and follows an AR(1) process with parameters ρ_{σ_ω} and σ_{σ_ω}. The second condition defines the return on capital, while the first one determines the spread between the expected return on capital and the riskless rate.[20] The following condition describes the evolution of entrepreneurial net worth:

$$\begin{aligned} n_t \;=\; & \zeta_{n,\tilde{R}^k}\left(\tilde{R}^k_t - \pi_t\right) - \zeta_{n,R}\left(R_{t-1} - \pi_t\right) + \zeta_{n,qK}\left(q^k_{t-1} + \bar{k}_{t-1}\right) + \zeta_{n,n} n_{t-1} \\ & - \frac{\zeta_{n,\sigma_\omega}}{\zeta_{sp,\sigma_\omega}} \tilde{\sigma}_{\omega,t-1}. \end{aligned} \tag{A-25}$$

State-Space Representation. The SWFF model uses in addition spreads as observables. The corresponding measurement equation is

$$\text{Spread} = SP_* + 100 I\!\!E_t\left[\tilde{R}^k_{t+1} - R_t\right], \tag{A-26}$$

where the parameter SP_* measures the steady state spread.

A.3 Prior Distribution

The prior distributions for the SWπ and the SWFF model are summarized in Table A-1. The joint prior distribution is obtained as the product of the marginals listed in the table.

[20] Note that if $\zeta_{sp,b} = 0$ and the financial friction shocks $\tilde{\sigma}_{\omega,t}$ are zero, (A-23) and (A-24) coincide with (A-6).

This prior is then truncated to ensure that for each parameter in the support of the prior the linearized DSGE model has a unique stable rational expectations equilibrium.

Table A-1: Priors

	Density	Mean	St. Dev.		Density	Mean	St. Dev.
Panel I: SWπ							
Policy Parameters							
ψ_1	Normal	1.50	0.25	ρ_R	Beta	0.75	0.10
ψ_2	Normal	0.12	0.05	ρ_{r^m}	Beta	0.50	0.20
ψ_3	Normal	0.12	0.05	σ_{r^m}	InvG	0.10	2.00
Nominal Rigidities Parameters							
ζ_p	Beta	0.50	0.10	ζ_w	Beta	0.50	0.10
Other "Endogenous Propagation and Steady State" Parameters							
α	Normal	0.30	0.05	π^*	Gamma	0.75	0.40
Φ	Normal	1.25	0.12	γ	Normal	0.40	0.10
h	Beta	0.70	0.10	S''	Normal	4.00	1.50
ν_l	Normal	2.00	0.75	σ_c	Normal	1.50	0.37
ι_p	Beta	0.50	0.15	ι_w	Beta	0.50	0.15
r_*	Gamma	0.25	0.10	ψ	Beta	0.50	0.15
(Note $\beta = (1/(1 + r_*/100))$)							
ρs, σs, and ηs							
ρ_z	Beta	0.50	0.20	σ_z	InvG	0.10	2.00
ρ_b	Beta	0.50	0.20	σ_b	InvG	0.10	2.00
ρ_{λ_f}	Beta	0.50	0.20	σ_{λ_f}	InvG	0.10	2.00
ρ_{λ_w}	Beta	0.50	0.20	σ_{λ_w}	InvG	0.10	2.00
ρ_μ	Beta	0.50	0.20	σ_μ	InvG	0.10	2.00
ρ_g	Beta	0.50	0.20	σ_g	InvG	0.10	2.00
η_{λ_f}	Beta	0.50	0.20	η_{λ_w}	Beta	0.50	0.20
η_{gz}	Beta	0.50	0.20				
ρ_{π^*}	Beta	0.50	0.20	σ_{π^*}	InvG	0.03	6.00
Panel II: SWFF							
SP_*	Gamma	2.00	0.10	$\zeta_{sp,b}$	Beta	0.05	0.005
ρ_{σ_w}	Beta	0.75	0.15	σ_{σ_w}	InvG	0.05	4.00

Notes: Smets and Wouters (2007) original prior is a $Gamma(.62, .10)$. The following parameters are fixed in Smets and Wouters (2007): $\delta = 0.025$, $g_* = 0.18$, $\lambda_w = 1.50$, $\varepsilon_w = 10$, and $\varepsilon_p = 10$. In addition, for the model with financial frictions we fix the entrepreneurs' steady state default probability $\bar{F}_* = 0.03$ and their survival rate $\gamma_* = 0.99$. The columns "Mean" and "St. Dev." list the means and the standard deviations for Beta, Gamma, and Normal distributions, and the values s and ν for the Inverse Gamma (InvG) distribution, where $p_{\mathcal{IG}}(\sigma|\nu, s) \propto \sigma^{-\nu-1} e^{-\nu s^2/2\sigma^2}$. The effective prior is truncated at the boundary of the determinacy region. The prior for $\bar{l}$ is $\mathcal{N}(-45, 5^2)$.

B Data

Real GDP (GDPC), the GDP price deflator (GDPDEF), nominal personal consumption expenditures (PCEC), and nominal fixed private investment (FPI) are constructed at a quarterly frequency by the Bureau of Economic Analysis (BEA), and are included in the National Income and Product Accounts (NIPA). Average weekly hours of production and nonsupervisory employees for total private industries (AWHNONAG), civilian employment (CE16OV), and civilian noninstitutional population (LNSINDEX) are produced by the Bureau of Labor Statistics (BLS) at the monthly frequency. The first of these series is obtained from the Establishment Survey, and the remaining from the Household Survey. Both surveys are released in the BLS Employment Situation Summary (ESS). Since our models are estimated on quarterly data, we take averages of the monthly data. Compensation per hour for the nonfarm business sector (COMPNFB) is obtained from the Labor Productvity and Costs (LPC) release, and produced by the BLS at the quarterly frequency. All data are transformed following Smets and Wouters (2007). Let Δ denote the temporal difference operator. Then:

$$
\begin{aligned}
\textit{Output growth} &= 100 * \Delta LN((GDPC)/LNSINDEX) \\
\textit{Consumption growth} &= 100 * \Delta LN((PCEC/GDPDEF)/LNSINDEX) \\
\textit{Investment growth} &= 100 * \Delta LN((FPI/GDPDEF)/LNSINDEX) \\
\textit{Real Wage growth} &= 100 * \Delta LN(COMPNFB/GDPDEF) \\
\textit{Hours} &= 100 * LN((AWHNONAG * CE16OV/100)/LNSINDEX) \\
\textit{Inflation} &= 100 * \Delta LN(GDPDEF).
\end{aligned}
$$

The federal funds rate is obtained from the Federal Reserve Board's H.15 release at the business day frequency. We take quarterly averages of the annualized daily data and divide by four. In the estimation of the DSGE model with financial frictions we measure *Spread* as the annualized Moody's Seasoned Baa Corporate Bond Yield spread over the 10-Year Treasury Note Yield at Constant Maturity. Both series are available from the Federal Reserve Board's H.15 release. Like the federal funds rate, the spread data is also averaged over each quarter and measured at the quarterly frequency. This leads to:

$$
\begin{aligned}
\textit{FFR} &= (1/4) * FEDERAL\ FUNDS\ RATE \\
\textit{Spread} &= (1/4) * (BaaCorporate\ -\ 10yearTreasury)
\end{aligned}
$$

The long-run inflation expectations are obtained from the Blue Chip Economic Indicators survey and the Survey of Professional Forecasters (SPF) available from the FRB Philadelphia's Real-Time Data Research Center. Long-run inflation expectations (average CPI inflation over the next 10 years) are available from 1991:Q4 onwards. Prior to 1991:Q4, we use the 10-year expectations data from the Blue Chip survey to construct a long time series that begins in 1979:Q4. Since the Blue Chip survey reports long-run inflation expectations only twice a year, we treat these expectations in the remaining quarters as missing observations and adjust the measurement equation of the Kalman filter accordingly. Long-run inflation expectations $\pi_t^{O,40}$ are therefore measured as

$$\pi_t^{O,40} = (\text{10-YEAR AVERAGE CPI INFLATION FORECAST} - 0.50)/4.$$

where 0.50 is the average difference between CPI and GDP annualized inflation from the beginning of the sample to 1992. We divide by 4 because the data are expressed in quarterly terms.

Many macroeconomic time series get revised multiple times by the statistical agencies that publish the series. In many cases the revisions reflect additional information that has been collected by the agencies, in other instances revisions are caused by changes in definitions. For instance, the BEA publishes three releases of quarterly GDP in the first three month following the quarter. Thus, in order to be able to compare DSGE model forecasts to real-time forecasts made by private-sector professional forecasters or the Federal Reserve Board, it is important to construct vintages of real time historical data. We follow the work by Edge and Gürkaynak (2010) and construct data vintages that are aligned with the publication dates of the Blue Chip survey. A detailed description of how this data set is constructed is provided in Del Negro and Schorfheide (2013).

C Computational Details

C.1 DSGE Models

The parameter estimation for the two DSGE models is described in detail in Del Negro and Schorfheide (2013). Thus, this Appendix focuses on the computation of h-step predictive densities $p(y_{t:t+h}|\mathcal{I}^m_{t-1}, \mathcal{M}_m)$. Starting point is the state-space representation of the DSGE model. The transition equation

$$s_t = \mathcal{T}(\theta)s_{t-1} + \mathcal{R}(\theta)\epsilon_t,\ \ \epsilon_t \sim N(0, \mathcal{Q}) \tag{A-27}$$

summarizes the evolution of the states s_t. The measurement equation:

$$y_t = \mathcal{Z}(\theta)s_t + \mathcal{D}(\theta), \tag{A-28}$$

maps the states onto the vector of observables y_t, where $\mathcal{D}(\theta)$ represents the vector of steady states for these observables. To simplify the notation we omit model superscripts/subscripts and we drop $\mathcal{M}_m$ from the conditioning set. We assume that the forecasts are based on the $\mathcal{I}_{t-1}$ information set. Let θ denote the vector of DSGE model parameters. For each draw θ^i, $i = 1, \dots, N$, from the posterior distribution $p(\theta|\mathcal{I}_{t-1})$, execute the following steps:

1. Evaluate
   $\mathcal{T}(\theta), \mathcal{R}(\theta), \mathcal{Z}(\theta), \mathcal{D}(\theta)$.

2. Run the Kalman filter to obtain $s_{t-1|t-1}$ and $P_{t-1|t-1}$.

3. Compute $\hat{s}_{t|t-1} = s_{t|\mathcal{I}_{t-1}}$ and $\hat{P}_{t|t-1} = P_{t|\mathcal{I}_{t-1}}$ as

   (a) Unconditional forecasts: $\hat{s}_{t|t-1} = \mathcal{T}s_{t-1|t-1}$, $\hat{P}_{t|t-1} = \mathcal{T}P_{t-1|t-1}\mathcal{T}' + \mathcal{R}\mathcal{Q}\mathcal{R}'$.

   (b) Semiconditional forecasts (using time t spreads, and FFR): after computing $\hat{s}_{t|t-1}$ and $\hat{P}_{t|t-1}$ using the "unconditional" formulas, run time t updating step of Kalman filter using a measurement equation that only uses time t values of these two observables.

4. Compute recursively for $j = 1,..,h$ the objects $\hat{s}_{t+j|t-1} = \mathcal{T} s_{t+j-1|t-1}$, $\hat{P}_{t+j|t-1} = \mathcal{T} P_{t+j-1|t-1} \mathcal{T}' + \mathcal{R}\mathcal{Q}\mathcal{R}'$ and construct the matrices

$$\hat{s}_{t:t+k|t-1} = \begin{bmatrix} \hat{s}_{t|t-1} \\ \vdots \\ \hat{s}_{t+k|t-1} \end{bmatrix}$$

and

$$\hat{P}_{t:t+k|t-1} = \begin{bmatrix} \hat{P}_{t|t-1} & \hat{P}_{t|t-1}\mathcal{T}' & \dots & \hat{P}_{t|t-1}\mathcal{T}^{k\ \prime} \\ \mathcal{T}\hat{P}_{t|t-1} & \hat{P}_{t+1|t-1} & \dots & \hat{P}_{t+1|t-1}\mathcal{T}^{k-1\ \prime} \\ \vdots & \vdots & \ddots & \vdots \\ \mathcal{T}^k\hat{P}_{t|t-1} & \mathcal{T}^{k-1}\hat{P}_{t+1|t-1} & \dots & \hat{P}_{t+k|t-1} \end{bmatrix}.$$

This leads to: $s_{t:t+h}|(\theta, \mathcal{I}_{t-1}) \sim N(\hat{s}_{t:t+h|t-1}, \hat{P}_{t:t+h|t-1})$.

5. The distribution of $y_{t:t+h} = \tilde{\mathcal{D}} + \tilde{\mathcal{Z}} s_{t:t+h}$ is

$$y_{t:t+h}|(\theta, \mathcal{I}_{t-1}) \sim N(\tilde{\mathcal{D}} + \tilde{\mathcal{Z}}\hat{s}_{t:t+h|t-1}, \tilde{\mathcal{Z}}\hat{P}_{t:t+h|t-1}\tilde{\mathcal{Z}}'),$$

where $\tilde{\mathcal{Z}} = I_{h+1} \otimes \mathcal{Z}$ and $\tilde{\mathcal{D}} = 1_{h+1} \otimes \mathcal{D}$ (note $I_1 = 1_1 = 1$)

6. Compute

$$p(y^o_{t:t+h}|\theta, \mathcal{I}_{t-1}) = p_N(y^o_{t:t+h}; \tilde{\mathcal{D}} + \tilde{\mathcal{Z}}\hat{s}_{t:t+h|t-1}, \tilde{\mathcal{Z}}\hat{P}_{t:t+h|t-1}\tilde{\mathcal{Z}}'), \tag{A-29}$$

where $y^o_{t:t+h}$ are the actual observations and $p_N(x; \mu, \Sigma)$ is the probability density function of a $N(\mu, \Sigma)$.

7. For linear functions $Fy_{t:t+h}$ (e.g., four quarter averages, etc.) where F is a matrix of fixed coefficients the predictive density becomes

$$p(Fy^o_{t:t+h}|\theta, \mathcal{I}_{t-1}) = p_N(Fy^o_{t:t+h}; F\tilde{\mathcal{D}} + F\tilde{\mathcal{Z}}\hat{s}_{t:t+h|t-1}, F\tilde{\mathcal{Z}}\hat{P}_{t:t+h|t-1}\tilde{\mathcal{Z}}'F'). \tag{A-30}$$

In the application we choose the matrix F such that $Fy_{t:t+h} = \bar{y}_{t+h,h} = \frac{1}{h}\sum_{j=1}^{h} y_{t+j}$ and let

$$p(\bar{y}^o_{t+h,h}|\mathcal{I}_{t-1}) = \frac{1}{N}\sum_{i=1}^{N} p(\bar{y}^o_{t+h,h}|\theta^i, \mathcal{I}_{t-1}). \tag{A-31}$$

C.2 Dynamic Prediction Pool

In each period t, the principal has to conduct inference about λ_t to generate $\hat{\lambda}^{DP}_{t+h|t}(\theta)$, where $\theta = (\rho, \mu, \sigma)'$ is the vector of hyperparameters. Some of the results that we are reporting in the main part of the paper are conditional on a particular value of θ, while others are obtained by integrating out θ under the relevant pseudo posterior distribution.

We use a bootstrap particle filter to update the sequence of pseudo posteriors $p^{(h)}(\lambda_t|\theta, \mathcal{I}^{\mathcal{P}}_t, \mathcal{P})$. Recent surveys of particle-filtering methods for nonlinear state-space models in econometrics are provided by Giordani et al. (2011), Creal (2012), and Herbst and Schorfheide (2016). Let $s_t = [x_t, \lambda_t]'$ and assume that the period $t-1$ particles $\{s^j_{t-1}, W^j_{t-1}\}^N_{j=1}$ approximate the moments of $p^{(h)}(\lambda_{t-1}|\theta, \mathcal{I}^{\mathcal{P}}_{t-1}, \mathcal{P})$:

$$\frac{1}{N}\sum_{j=1}^{N} f(s^j_{t-1})W^j_{t-1} \approx \int f(s_{t-1})p^{(h)}(s_{t-1}|\theta, \mathcal{I}^{\mathcal{P}}_{t-1}, \mathcal{P})ds_{t-1}. \tag{A-32}$$

By $\approx$ we mean that under suitable regularity conditions (see, for instance, Chopin (2004)) the Monte Carlo average satisfies a strong law of large numbers and a central limit theorem. An initial set of particles can be generated by *iid* sampling from $x_0 \sim N(\mu, \sigma^2)$, letting $s^j_0 = [x^j_0, \Phi(x^j_0)]$, and setting $W^j_0 = 1$. The bootstrap particle filter involves the following recursion:

1. Propagate particles forward:

$$\tilde{x}^j_t = (1-\rho)\mu + \rho x^j_{t-1} + \sqrt{1-\rho^2}\sigma\varepsilon^j_t, \;\; \varepsilon^j_t \sim N(0,1). \tag{A-33}$$

2. Compute $\tilde{\lambda}^j_t = \Phi(\tilde{x}^j_t)$ and let $\tilde{s}^j_t = [\tilde{x}^j_t, \tilde{\lambda}^j_t]'$.

3. Compute the incremental weights

$$\tilde{w}^j_t = p^{(h)}(\bar{y}_{t,h}|\lambda^j_t, \mathcal{I}^{\mathcal{P}}_{t-1}, \mathcal{P}) = \tilde{\lambda}^j_t p(\bar{y}_{t,h}|\mathcal{I}^1_{t-h}, \mathcal{M}_1) + (1-\tilde{\lambda}^j_t)p(\bar{y}_{t,h}|\mathcal{I}^2_{t-h}, \mathcal{M}_2). \tag{A-34}$$

The predictive density $p^{(h)}(\bar{y}_{t,h}|\theta, \mathcal{I}^{\mathcal{P}}_{t-1}, \mathcal{P})$ can be approximated by

$$\hat{p}^{(h)}(\bar{y}_{t,h}|\theta, \mathcal{I}^{\mathcal{P}}_{t-1}, \mathcal{P}) = \frac{1}{N}\sum_{j=1}^{N} \tilde{w}^j_t W^j_{t-1}. \tag{A-35}$$

4. Update the weights according to

$$\tilde{W}_t^j = \frac{\tilde{w}_t^j W_{t-1}^j}{\frac{1}{N}\sum_{j=1}^N W_{t-1}^j}. \tag{A-36}$$

5. Resample (using multinomial resampling) the particles if the distribution of particle weights becomes very uneven. Let $ESS = N^2/\sum_{j=1}^N \tilde{w}_t^j W_{t-1}^j$. (a) If $ESS < (2/3)N$ resample the particles and let s_t^j denote the value of the resampled particle j and set its weight $W_t^j = 1$. (b) If $ESS \geq (2/3)N$ let $s_t^j = \tilde{s}_t^j$ and $W_t^j = \tilde{W}_t^j$.

6. The particle system $\{s_t^j, W_t^j\}_{j=1}^N$ approximates

$$\text{plim}_{N \longrightarrow \infty} \frac{1}{N}\sum_{j=1}^N f(s_{t-1}^j) W_{t-1}^j = \int f(s_{t-1}) p^{(h)}(s_{t-1}|\theta, \mathcal{I}_{t-1}^{\mathcal{P}}, \mathcal{P}) ds_{t-1} \tag{A-37}$$

In Figure A-1 we graphically examine the Monte Carlo variance of our estimate of $p^{(h)}(\lambda_t|\theta, \mathcal{I}_t^{\mathcal{P}}, \mathcal{P})$. The figure is based on $N = 1,000$ particles and $N_{rep} = 100$ independent runs of the particle filter. We set $\rho = 0.9$, $\mu = 0$, and $\sigma = 1$. The accuracy deteriorates somewhat as ρ approaches one, because the innovation in state-transition equation decreases and do does the degree of particle mutation. For the limit case $\rho = 1$ filtering becomes unnecessary because $\lambda_t = \lambda$.

The predictive densities can be combined to form the pseudo-likelihood function

$$p^{(h)}(\bar{y}_{1:t,h}|\theta, \mathcal{P}) = \prod_{t=1}^T p^{(h)}(\bar{y}_{t,h}|\theta, \mathcal{I}_{t-1}^{\mathcal{P}}, \mathcal{P}). \tag{A-38}$$

The pseudo-likelihood has the particle filter approximation

$$\hat{p}^{(h)}(\bar{y}_{1:t,h}|\theta, \mathcal{P}) = \prod_{t=1}^T \hat{p}^{(h)}(\bar{y}_{t,h}|\theta, \mathcal{I}_{t-1}^{\mathcal{P}}, \mathcal{P}), \tag{A-39}$$

where $\hat{p}^{(h)}(\bar{y}_{t,h}|\theta, \mathcal{I}_{t-1}^{\mathcal{P}}, \mathcal{P})$ was defined in (A-35). We use the pseudo-likelihood function to conduct inference with respect to θ:

$$p^{(h)}(\theta|\mathcal{I}_t^{\mathcal{P}}, \mathcal{P}) \propto \hat{p}^{(h)}(\bar{y}_{1:t,h}|\theta, \mathcal{P}) p(\theta). \tag{A-40}$$

In order to generate draws from pseudo-posterior $p^{(h)}(\theta|\mathcal{I}_t^{\mathcal{P}}, \mathcal{P})$, we embedd the particle-filter approximation of the pseudo-likelihood function in an otherwise standard random-walk

Figure A-1: Accuracy of Particle Filter Approximation: $N = 1000$, $N_{rep} = 100$

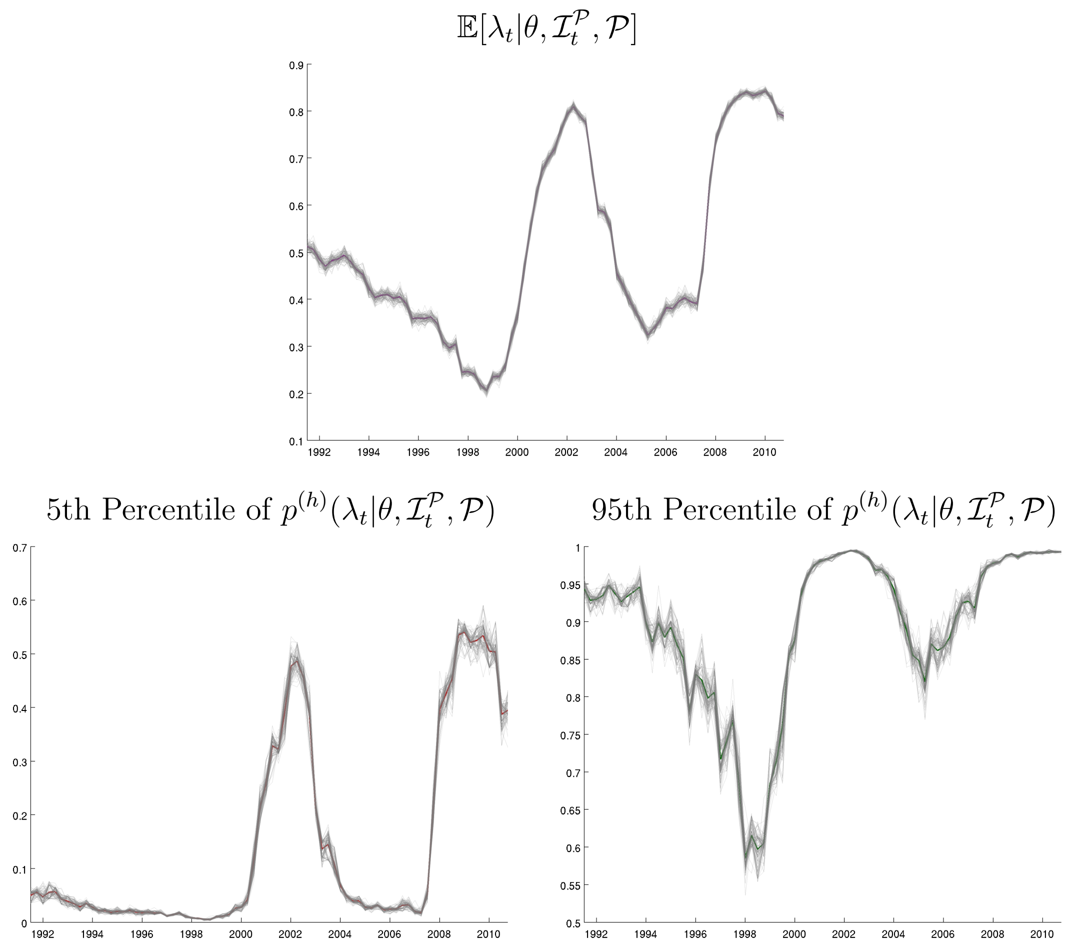

Notes: Figure depicts results from N_rep runs of the particle filter. θ is given by $\rho = 0.9$, $\mu = 0$, and $\sigma = 1$.

Metropolis-Hastings algorithm. A theoretical justification for this procedure is provided in Andrieu et al. (2010). The random-walk Metropolis-Hastings (RWMH) algorithm is identical to Algorithm 1 in Del Negro and Schorfheide (2013). Due to the low dimensionality of the hyperparameter vector θ and the high degree of accuracy of the particle filter approximation, the posterior sampler is very efficient. All results reported in the main text are based on 5,000 particles and 10,000 draws from the RWMH algorithm.

D Additional Tables and Figures

D.1 Posterior Distribution of Hyperparameters

Figure A-2: Posterior $p^{(h)}(\rho|\mathcal{I}_t^{\mathcal{P}}, \mathcal{P})$ Over Time

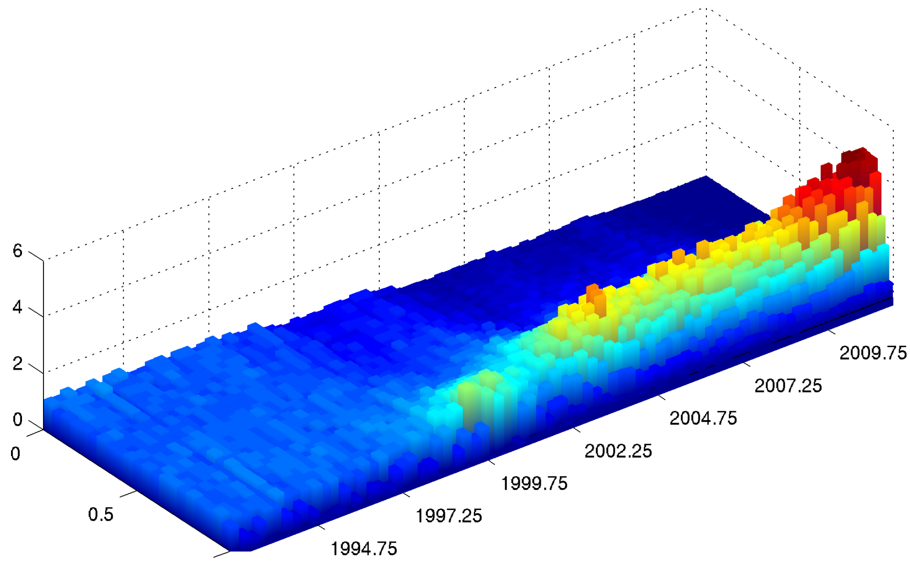

Notes: The figure shows the posterior $p^{(h)}(\rho|\mathcal{I}_t^{\mathcal{P}}, \mathcal{P})$ for t =1992:Q1-2011:Q2 based on the hyperparameter Prior 1: $\rho \sim \mathcal{U}[0,1]$, $\mu = 0$, $\sigma = 1$.

Figure A-3: End-of-Sample Posterior of the Hyperparameter ρ Under Different Priors

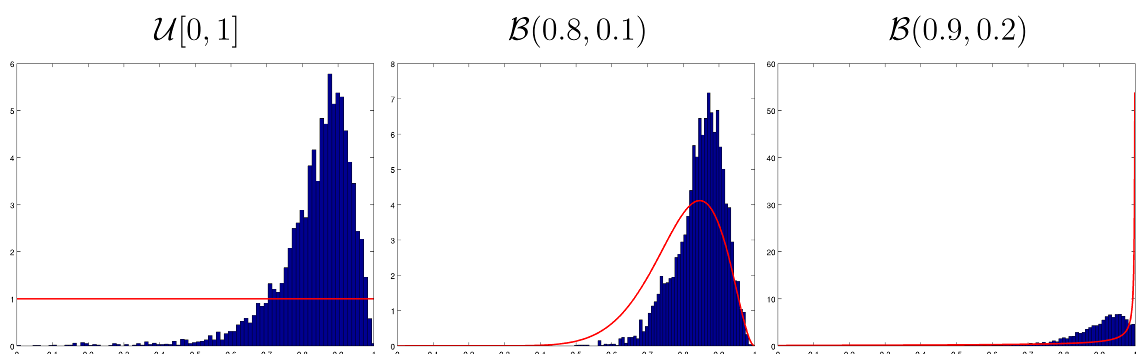

Notes: The three panels show the posterior $p(\rho|\mathcal{I}_T^{\mathcal{P}}, \mathcal{P})$ (histogram) under three priors (red line): $\mathcal{U}[0,1]$, $\mu = 0$, $\sigma = 1$ (left); $\rho \sim \mathcal{B}(0.8, 0.1)$, $\mu \sim \mathcal{N}(0, \Phi^{-1}(0.75))$, $\sigma^2 \sim \mathcal{IG}(2,1)$ (center); and $\mathcal{B}(0.9, 0.2)$, $\mu \sim \mathcal{N}(0, \Phi^{-1}(0.75))$, $\sigma^2 \sim \mathcal{IG}(2,1)$ (right).

D.2 Cumulative Log Scores Over Time

Figure A-4: Cumulative Log Scores Over Time: SWFF and SWπ vs Dynamic Pools

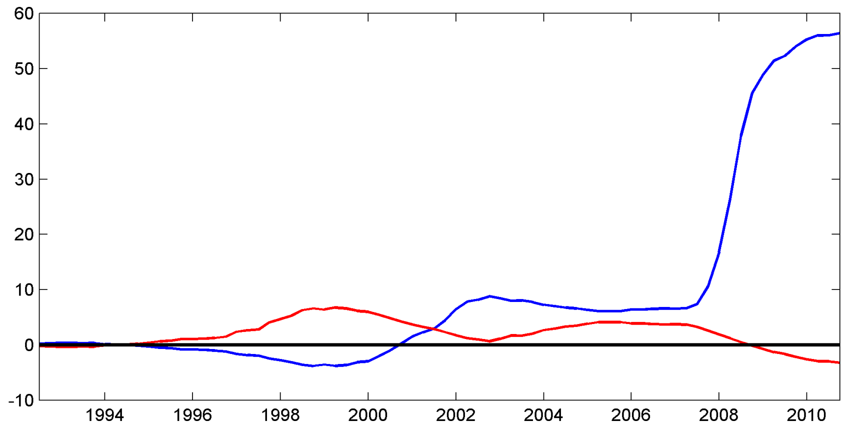

Notes: The figure shows shows the difference between the cumulative log scores $\sum_{t=1}^{\tau} \ln p(\bar{y}_{t+h,h}|\mathcal{I}_{t+}^{m}, \mathcal{M}_m)$ of the SWFF (red) and SWπ (blue) models, respectively, and the cumulative log score for the dynamic pools (black) $\sum_{t=1}^{\tau} \ln p_{DP}^{(h)}(\bar{y}_{t+h,h}|\mathcal{I}_{t+}^{\mathcal{P}}, \mathcal{P})$ over the period 1993:Q1-2011:Q2. We use Prior 1 for the DP: $\rho \sim \mathcal{B}(0.8, 0.1)$, $\mu = 0$, $\sigma^2 = 1$.

D.3 Results from Dynamic Model Averaging (DMA)

Figure A-5: Weights in Realtime: DMA ($\alpha = 0.90, 0.95, 0.99$) vs. DP

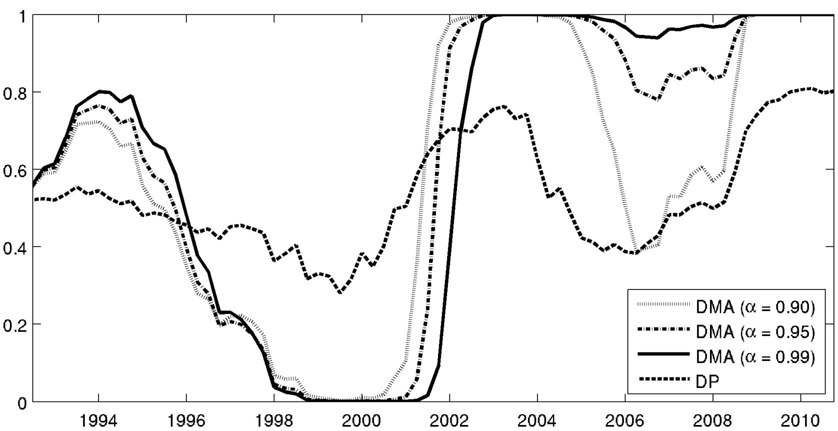

Notes: The figure shows the weight on the SWFF model in forecast pools over the period 1992:Q1-2011:Q2 for Dynamic Model Averaging (DMA) for three values of α: .99, .95, and .90, as well as the dynamic pool weight ($\hat{\lambda}^{DP}_{t|t}$). Prior 1 is used for the DP: $\rho \sim \mathcal{U}[0,1]$, $\mu = 0$, $\sigma = 1$.

Table A-2: Cumulative Log Scores / Differentials

DP Prior	Log Score DP (1)	Differentials $\alpha = 0.90$ (2)	$\alpha = 0.95$ (3)	$\alpha = 0.99$ (4)
Prior 1: $\rho \sim U(0,1)$, $\mu = 0$, $\sigma^2 = 1$	-256.91	-0.12	0.33	2.74
Prior 2: $\rho \sim \mathcal{B}(0.8, 0.1)$, $\mu \sim \mathcal{N}(0, \Phi^{-1}(.75))$, $\sigma^2 \sim \mathcal{IG}(2,1)$	-256.43	0.36	0.81	3.22
Prior 3: $\rho \sim \mathcal{B}(0.8, 0.1)$, $\mu = 0$, $\sigma^2 \sim \mathcal{IG}(2,1)$	-255.97	0.82	1.27	3.68

Notes: The table shows in column (1) the cumulative log score $\sum_{t=1}^{T} \ln p^{(h)}_{DP}(\bar{y}_{t+h,h} | \mathcal{I}^{\mathcal{P}}_{t^+}, \mathcal{P})$ for various specifications of the dynamic pool. Columns (2) through (4) show for each specification the difference between the DP cumulative log scores and that of DMA for $\alpha = 0.90$, 0.95, and 0.99, respectively. The cumulative log scores are computed over the period 1992:Q1-2011:Q2.

D.4 Robustness Check: Omit Information from $t + 1$ Financial Variables

Figure A-6: Log Scores Comparison: SWFF vs. SWπ Without Time $t+1$ Information from Financial Variables

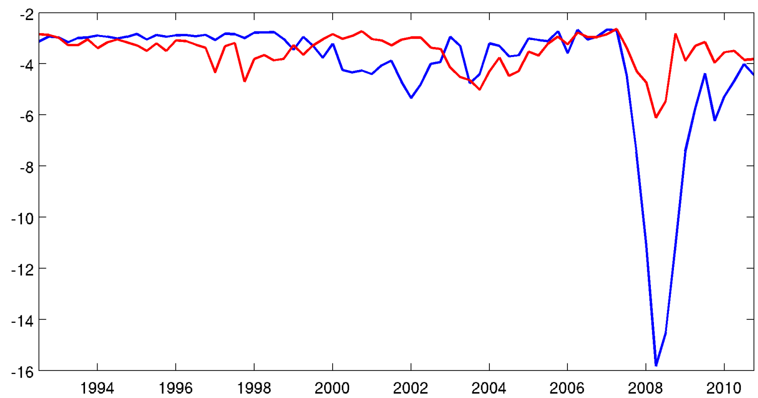

Notes: The figure shows the log scores $p(\bar{y}_{t+h,h}|\mathcal{I}_t^m, \mathcal{M}_m)$ for SWFF (red), and SWπ (blue) over the period 1992:Q1-2011:Q2.

Figure A-7: Weights in Real Time: BMA, Static, and Dynamic Pools – $\mathcal{I}_t^m$ Excludes Time $t+1$ Information from Financial Variables

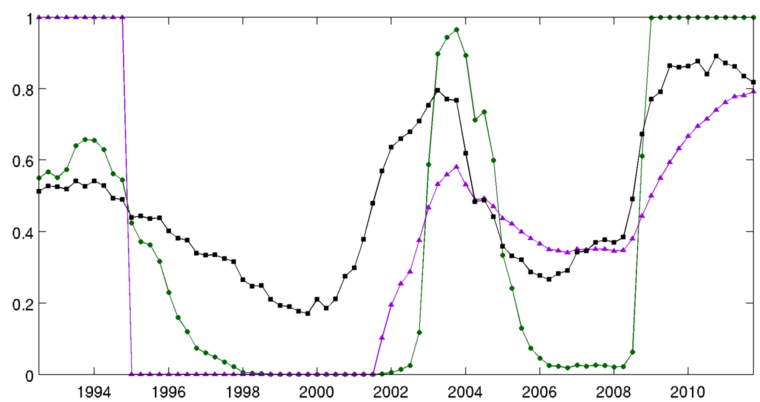

Notes: The figure shows the weight on the SWFF model in forecast pools, computed using real time information only, over the period 1992:Q1-2011:Q2 for three different pooling techniques: BMA ($\hat{\lambda}_t^{BMA}$ – green), (maximum likelihood) static pool ($\hat{\lambda}_t^{MSP}$ – purple), and dynamic pools ($\hat{\lambda}_{t|t}^{DP}$ – black).

D.5 Robustness Check: Individual Forecasts

The main part of the paper focuses on the joint prediction of output growth and inflation, because it is their joint behavior that is arguably most of interest to policymakers. Nonetheless we want to briefly describe the results obtained when applying our methodology to semi-conditional forecasts of four-quarter-ahead averages of each variable separately. Detailed results are presented in Figure A-8. First, the discrepancy in log predictive scores for the two models is larger for output growth than for inflation, and as a consequence the time series behavior of the joint predictive likelihood is largely driven by the former. Second, the evolution of the weight given to the SWFF model by the DP approach is qualitatively similar for output growth and inflation: The weight rises in the aftermath of the dot-com bust in the 2000s and over the subsequent period of financial turmoil, decreases in the mid-2000s, and then rises again with the financial crisis leading to the Great Recession. The pattern for output and inflation differ a bit in the 1990s, when the SWFF model performs slightly better than the SWπ model for inflation but not for output, and after 2009, when the opposite occurs.

Third, the BMA weights, and to a lesser extent the MSP weights, also tend to approach the extremes of zero or one as enough information accumulates favoring one model versus the other. For instance, by the end of the 1990s both the BMA and the MSP weight are zero for output growth. For inflation, by the end of the early 2000s financial turmoil period both weights are one. Before 2008, there appears to be a negative correlation among the BMA and MSP weights for output growth and inflation. In periods in which the output growth weights favor the SWπ model, the inflation weights favor the SWFF model and vice versa. Fourth, this “lack of diversification” penalizes both BMA and MSP relative to DP when the environment changes, resulting in large losses in terms of predictive densities. For both output and inflation the performance of the dynamic pools is close to that of equal weights.

Figure A-8: Results for Individual Variables

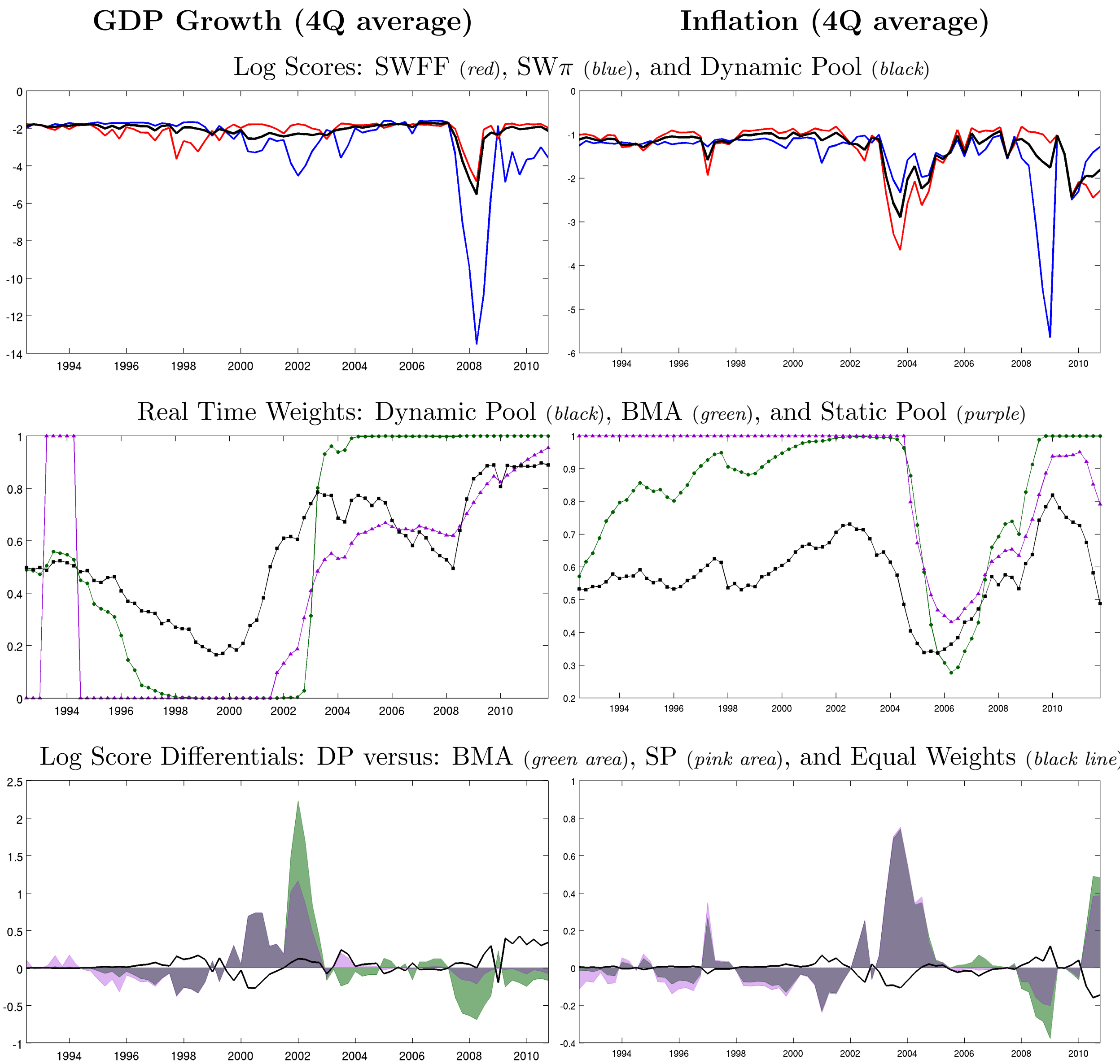

Notes: The left and right column shows the results for the 4-quarter average output growth and inflation, respectively. We use Prior 2 for the DP: $\rho \sim \mathcal{B}(0.8, 0.1)$, $\mu \sim \mathcal{N}(0, \Phi^{-1}(0.75))$, $\sigma^2 \sim \mathcal{IG}(2, 1)$. Top panels: log scores $\ln p(\bar{y}_{t+h,h}|\mathcal{I}^m_{t+}, \mathcal{M}_m)$ for SWFF, and SWπ, and log score $\ln p^{(h)}_{DP}(\bar{y}_{t+h,h}|\mathcal{I}^{\mathcal{P}}_{t+}, \mathcal{P})$ for the dynamic pool (DP). Middle panels: real time weights on the SWFF model: DP ($\hat{\lambda}^{DP}_{t|t}$), static pool ($\hat{\lambda}^{MSP}_t$), and BMA ($\hat{\lambda}^{BMA}_t$). Bottom panels: log score differences of DP versus BMA ($\ln p^{(h)}_{BMA}(\bar{y}_{t+h,h}|\mathcal{I}^{\mathcal{P}}_{t+}, \mathcal{P})$), static pool ($\ln p^{(h)}_{MSP}(\bar{y}_{t+h,h}|\mathcal{I}^{\mathcal{P}}_{t+}, \mathcal{P})$), and equal weights. Positive values favor DP.

D.6 Robustness Check: One-Step-Ahead Forecasting

Figure A-9: Log Scores Comparison over Time for One-Quarter Ahead Forecasts

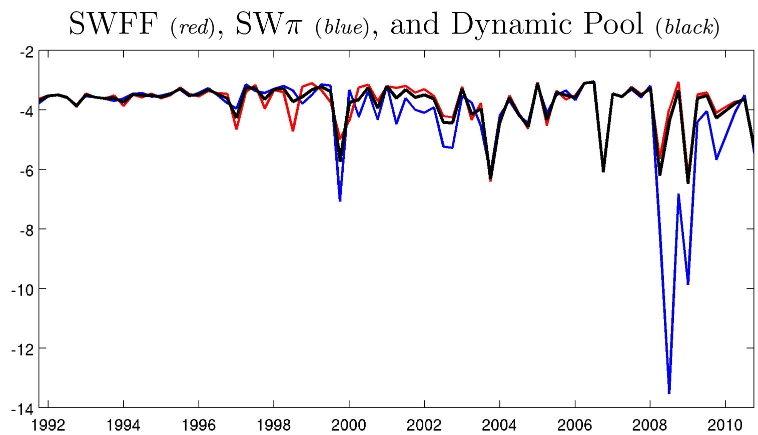

Notes: The figure shows the log scores $\ln p(\bar{y}_{t+h,h}|\mathcal{I}^m_{t+}, \mathcal{M}_m)$ for SWFF (red), and SWπ (blue), and the log score for the dynamic pools (black) $\ln p^{(h)}_{DP}(\bar{y}_{t+h,h}|\mathcal{I}^{\mathcal{P}}_{t+}, \mathcal{P})$ over the period 1992:Q1-2011:Q2. For the DP we set $\rho = .9$.